Delivery of Molecular and Nanoscale Medicine to Tumors: Transport Barriers and Strategies

Vikash P. Chauhan,[1,2] Triantafyllos Stylianopoulos,[1] Yves Boucher,[1] and Rakesh K. Jain[1]

[1]Edwin L. Steele Laboratory, Department of Radiation Oncology, Massachusetts General Hospital and Harvard Medical School, Boston, Massachusetts 02114; email: jain@steele.mgh.harvard.edu

[2]Harvard School of Engineering and Applied Sciences, Harvard University, Cambridge, Massachusetts 02138

Annu. Rev. Chem. Biomol. Eng. 2011. 2:281–98

The *Annual Review of Chemical and Biomolecular Engineering* is online at chembioeng.annualreviews.org

This article's doi:
10.1146/annurev-chembioeng-061010-114300

1947-5438/11/0715-0281$20.00

Keywords

cancer, microenvironment, drug resistance, normalization

Abstract

Tumors are similar to organs, with unique physiology giving rise to an unusual set of transport barriers to drug delivery. Cancer therapy is limited by nonuniform drug delivery via blood vessels, inhomogeneous drug transport into tumor interstitium from the vascular compartment, and hindered transport through tumor interstitium to the target cells. Four major abnormal physical and physiological properties contribute to these transport barriers. Accumulated solid stress compresses blood vessels to diminish the drug supply to many tumor regions. Immature vasculature with high viscous and geometric resistances and reduced pressure gradients leads to sluggish and heterogeneous blood flow in tumors to further limit drug supply. Nonfunctional lymphatics coupled with highly permeable blood vessels result in elevated hydrostatic pressure in tumors to abrogate convective drug transport from blood vessels into and throughout most of the tumor tissue. Finally, a dense structure of interstitial matrix and cells serves as a tortuous, viscous, and steric barrier to diffusion of therapeutic agents. In this review, we discuss the origins and implications of these barriers. We then highlight strategies for overcoming these barriers by modulating either drug properties or the tumor microenvironment itself to enhance the delivery and effectiveness of drugs in tumors.

INTRODUCTION

Cancer is a systemic disease, with more than 90% of cancer-related deaths caused by metastases, and thus it requires a systemic therapy. As such, efficient and uniform systemic drug delivery is a critical issue for the treatment of patients with advanced disease. A therapeutic agent for the treatment of cancer must follow a long and complex journey from the point of entry into the circulation to its target cells. Three major transport steps govern how effectively an agent will navigate this path: vascular transport, transvascular transport, and interstitial transport (1). These steps are highly efficient for typical normal tissues, as they evolved for effective oxygen and nutrient delivery. Unfortunately, the abnormal physiology of tumors gives rise to a set of transport barriers that limit the rate and extent of drug delivery to both primary and metastatic tumors.

Transport barriers to drug delivery arise from abnormal characteristics of the tumor microenvironment. The pathophysiological state of tumors consists of four major unusual properties: accumulated solid stress (2–5), abnormal blood vessel networks (6–13), elevated interstitial fluid pressure (14–17), and a dense interstitial structure (18–22). These abnormalities result in barriers to systemic drug delivery that exist in the form of variable avascular regions and sluggish blood flow leading to low and nonuniform perfusion rates in tumors, diminished transmural pressure gradients that limit transvascular transport to passive diffusion, highly viscoelastic interstitial components with tortuous paths and drug sequestration that hinder drug penetration by diffusion, and heterogeneity in the microenvironment that results in poor drug delivery. These transport barriers limit the distribution of molecules as small as oxygen (23, 24). As a result, the effectiveness of antitumor agents—from small-molecule chemotherapeutics to nanomedicines such as antibodies, oncolytic viruses, and nanoparticles—is diminished by the tumor microenvironment before these therapeutics reach their target cells (15, 24–26).

In this review, we present a physical sciences approach to drug delivery barriers in tumors. We discuss the key physiological abnormalities in tumors related to drug transport and demonstrate the impact of each. Finally, we summarize approaches to overcoming these physiological resistance mechanisms to molecular therapeutics and nanomedicines through normalization of the tumor microenvironment and modulation of drug properties.

DETERMINANTS OF DRUG TRANSPORT IN TUMORS

The delivery of cancer chemotherapeutics and nanomedicine involves transport steps that the pathophysiology of tumors generally hinders. Three important pharmacokinetic steps govern drug delivery to tumor cells and precede pharmacodynamic events, including transport and metabolism in cells—vascular transport, transvascular transport, and interstitial transport (**Figure 1**)—and each has its own set of transport barriers. To understand the biophysical underpinnings of these transport barriers, we must first develop a sense of these processes, clarify how they are studied, and determine the parameters that govern them.

Vascular Transport

Vascular transport, the supply of drugs via the blood into regions of the tumor, includes the flux of drugs or drug vehicles into a tumor and the distribution of these drugs to regions of the tumor via the tumor vascular network. Thus, vascular transport is quantified based on the perfusion rate of blood q, defined as the volumetric flow rate Q divided by the tissue volume V, or $q = \frac{Q}{V}$, to different regions of a tumor. The flow rate Q itself is equal to the pressure drop Δp divided by the resistance R, or $Q = \frac{\Delta p}{R}$, which has both viscous and geometric components. The relevant determinants of drug supply to tumor tissue are the flux of drug J_v into a tissue region by blood vessels, which

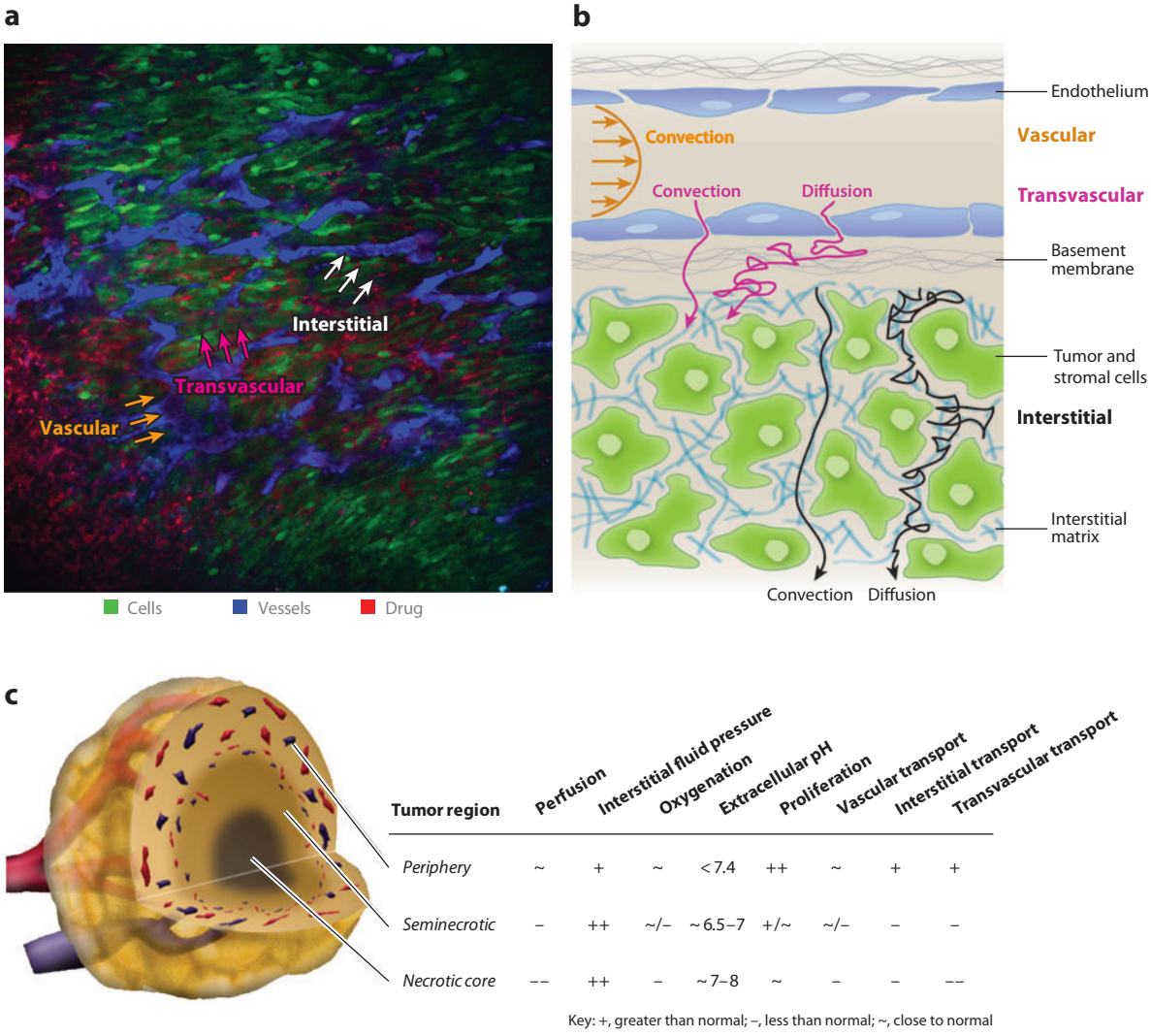

Figure 1

Transport in tumors. (*a*) A schematic of drug transport steps overlaid on an image of the tumor margin of an orthotopic mammary tumor in a mouse that depicts delivery of a low-molecular-weight fluorescent probe after 30 min. Overall, delivery is heterogeneous and poor, with retention of the probe in the peritumor tissue. Examples of vascular, transvascular, and interstitial transport steps are depicted. (*b*) Transport steps in a tumor tissue unit consisting of blood vessels and the surrounding tissue. (*c*) General properties of the tumor microenvironment, including drug delivery heterogeneity. Three regions of tumors—the periphery, seminecrotic region, and necrotic core—are delineated along with their characteristics. Adapted from Reference 122.

is equal to Q multiplied by the drug concentration in the feeding blood vessel C_v, or $J_v = QC_v$, along with the heterogeneity in vascular distributions and flow rates that determine the volume of distribution. This heterogeneity can be considered in terms of the distribution of perfusion rates, calculated as the volumetric flow rate for each vessel Q_j multiplied by the volume of tissue it feeds V_j. The parameters Q_j, C_j, and V_j can be measured in real time using standard intravital microscopy (8), multiphoton microscopy (7, 27), and potentially optical frequency domain imaging (28).

Transvascular Transport

Transvascular transport, the flux of drugs across vessel walls and their basement membranes, proceeds by a combination of diffusive and convective transport. Diffusive flux $J_{t,d}$ is dependent on the difference between the plasma concentration C_v and the interstitial concentration C_i multiplied by the vascular surface area S_v, with a constant of proportionality termed the vascular permeability P_t, or $J_{t,d} = P_t S_v(C_v - C_i)$. Similarly, convective flux $J_{t,a}$ is proportional to S_v times C_v multiplied by the difference between the transmural hydrostatic pressure gradient Δp_t and the osmotic reflection coefficient σ multiplied by the transmural osmotic pressure gradient $\Delta\Pi$, with the hydraulic conductivity K_t and the difference from unity of the solute's reflection coefficient σ_s as constants of proportionality, or $J_{t,a} = C_v K_t S_v(1 - \sigma_s)(\Delta p_t - \sigma\Delta\Pi)$. The combined transvascular flux J_t can then be expressed in terms of the Péclet number Pe, with $J_t = K_t S_v(1 - \sigma_s)(\Delta p_t - \sigma\Delta\Pi)\frac{C_v e^{Pe} - C_i}{e^{Pe} - 1}$. The permeability P_t and hydraulic conductivity K_t are dependent on the biophysical properties of the vessel wall and basement membrane, including their viscoelasticity and porosity, along with the physicochemical properties of the drug or drug carrier, including size, charge, and configuration. The transvascular flux J_t, equal to the sum of $J_{t,d}$ and $J_{t,a}$, can be measured using intravital microscopy (29, 30), including multiphoton microscopy-based methods (27), with fluorescent probes.

Interstitial Transport

Interstitial transport, the penetration and distribution of drugs through the tumor tissue toward their target cells following transvascular transport, also occurs through the combination of diffusive and convective transport. Diffusive transport in the interstitium, in terms of the change in concentration with time, is proportional to the interstitial concentration Laplacian $\nabla^2 C_i$, with the diffusion coefficient D as a proportionality constant, or $\frac{\partial C_i}{\partial t} = D\nabla^2 C_i$. Similarly, the change in concentration with time by convection is equal to the dot product of the interstitial fluid velocity v_i and concentration gradient ∇C_i, or $\frac{\partial C_i}{\partial t} = v_i \cdot \nabla C_i$. Furthermore, v_i is given as the product of the interstitial hydraulic conductivity K_i and hydrostatic pressure gradient ∇p_i, or $v_i = -K_i \nabla p_i$. D and K_i are determined by the properties of the interstitium, including the organization and concentration of interstitial macromolecules, and additionally are functions of drug or drug carrier properties such as size, charge, and configuration. Interstitial transport can be studied using intravital microscopy techniques, such as fluorescence recovery after photobleaching and fluorescence correlation spectroscopy (31–34), both of which have multiphoton microscopy-based approaches (18, 35–37).

Cell Transport and Metabolism

Cellular uptake, the last transport step for drugs that act on cells, is dependent on the properties of the drug itself in its interactions with the cell membrane and membrane molecules. These pharmacodynamic events are complex, with many different reactions to consider for binding and several modes of cell uptake and metabolism. Here we focus on the first three barriers, which can be studied properly only in vivo and therefore require innovative techniques to measure. Furthermore, cellular processes can be easily studied in vitro, though not all the resulting conclusions may translate in vivo.

PATHOPHYSIOLOGY CONTRIBUTING TO TRANSPORT BARRIERS

Abnormalities in the tumor microenvironment contribute to resistance to molecular and nanoscale medicine. Specifically, four critical abnormal physiological characteristics lead to diminished drug

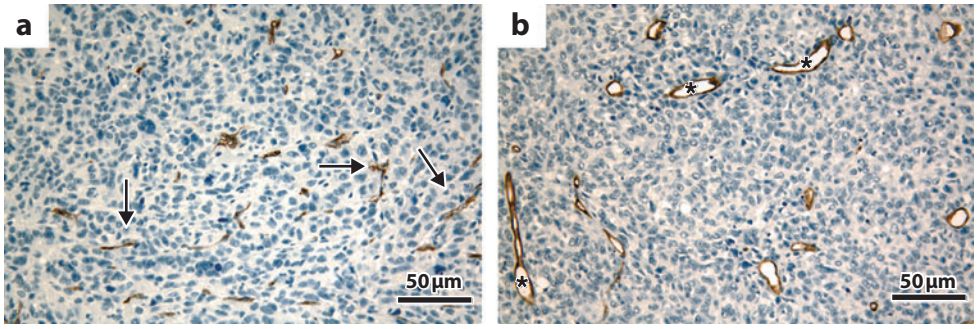

Figure 2

Growth-induced solid stress. (*a*) Solid stress from tumor cells compresses blood vessels and lymphatics, collapsing them (*arrows*). (*b*) Reducing solid stress by eliminating cancer cells with diphtheria toxin decompresses blood vessels (*asterisks*). This decompression improves perfused vessel fractions. Figure reproduced from Reference 5.

delivery and effectiveness in tumors. Each of these properties can limit multiple transport processes, leading to greatly hindered drug delivery. Furthermore, each has a set of cellular or molecular constituents that, through concerted actions, lead to system-level resistance.

Growth-Induced Solid Stress

Tumors are characterized by the uncontrolled proliferation and growth of cells in restricted space. Such unbridled tissue expansion builds solid stress through contact with normal neighboring cells and matrix components (3, 38), with the resulting force generation wreaking havoc on normal cell functions such as controlled proliferation and migration (3, 39). Within tumors, this solid stress accumulates through cellular hyperplasia and hyperproduction of interstitial matrix molecules such as collagen and hyaluronan. The result is the compression of blood and lymphatic vessels (**Figure 2**) (2, 5). As such, vascular density and perfusion rates in tumors tend to decrease with growth (40).

The accumulation of solid stress in tumors has two major consequences for drug transport aside from its effects on cellular function. First, the compression of blood vessels limits vascular transport by collapsing vessels and by slowing blood flow through increased vascular geometric resistance (11, 41). Thus, the solid stress–induced vascular changes limit drug distribution by poor perfusion to many tumor regions (13, 42). This poor perfusion compounds the drug supply issues by rendering the tumor microenvironment hypoxic, acidic, and necrotic (43), which can further contribute to drug resistance and disease progression. Second, the compression of lymphatic vessels in tumors renders them nonfunctional (4), which induces fluid retention within tumors (44). This fluid retention results in a flattening of the interstitial fluid pressure gradient (45, 46), which diminishes the driving force for convective interstitial transport. Therefore, the accumulation of solid stress leads to barriers to both vascular and interstitial transport.

Abnormal Blood Vessel Networks

Driven by genetic and epigenetic changes, tumor cells tend to produce a cocktail of proangiogenic factors (47). This allows tumors to grow beyond ~1–2 mm in size (48), a limit that exists largely due to the ~200-µm diffusion distance of oxygen and nutrients in tissue (43, 49, 50).

This overproduction of proangiogenic factors is uncontrolled and thus can be considered as constitutively active in angiogenic tumors and metastases (51). In contrast, normal angiogenesis during development and wound healing begins with production of proangiogenic factors, which induce vessel sprouting and growth. Normal angiogenesis then proceeds with a tapering of proangiogenic cytokine levels and increased antiangiogenic factor production, a balancing act that induces maturation of the new vessels (52, 53). Owing to the overactivation of proangiogenic pathways—such as the vascular endothelial growth factor (VEGF) pathway—in tumors, tumor vessels do not mature fully and instead remain tortuous and leaky (54).

The tortuous and leaky vessel combination leads to major consequences for tumor blood flow. Tumor vasculature typically lacks an orderly branching hierarchy and dependence of blood flow on vessel diameter, a general feature of normal microvasculature (13). The high tortuosity of tumor vessels contributes to an elevated geometric resistance, which slows blood flow (11). Considering that blood is generally a shear-thinning fluid, this drop in blood flow from geometric resistance has a great effect on the viscous resistance of blood in tumors (10). These immature tumor vessels are heterogeneously hyperpermeable to fluid and macromolecules owing to the presence of vessel wall fenestrae, transendothelial channels, and large pores disseminated throughout the vasculature (55–57). Vessel tortuosity and high permeability couple to contribute to a localized slowing of blood flow owing to fluid loss that increases the hematocrit of tumor blood to further elevate its viscosity (9, 10, 58). This combination of effects makes the abnormal tumor vascular network a major barrier to vascular transport; tumor blood flow can be up to an order of magnitude slower than in the surrounding normal tissue (**Figure 3**) (12).

Elevated Interstitial Fluid Pressure

The concerted effects of the nonfunctional lymphatics and hyperpermeable blood vessels result in an accumulation of fluid and plasma macromolecules in the tumor interstitium. With no drainage and no transmural difference in oncotic pressure, the interstitial fluid pressure rises to the level of the microvascular pressure (**Figure 4**) (14, 59). The leaky vasculature ensures that the interstitial fluid pressure tracks with microvascular pressure changes with a delay on the order of 10 s. The absence of lymphatic drainage, together with large interstitial transport distances and low interstitial hydraulic conductivity, makes the fluid clearance time on the order of 10^3 s (17). As a result, the transvascular and interstitial fluid pressure gradients in tumors are effectively zero (14, 45), except at the tumor margins, where peritumoral lymphatics drain the excess fluid (4, 16, 46, 60).

With no fluid pressure gradients, the driving force for convective mass transport is effectively abrogated, leaving diffusion largely responsible for the transvascular and interstitial transport of drugs and drug carriers in the bulk of tumors. Combined with the large volumes that each

Figure 3

Abnormal blood vessel networks. (*a*) The vascular network of a brain tumor in mice in comparison with peritumoral vessels and normal vessels on the contralateral side of the brain. Tumor vessels are more tortuous and wider than normal vessels, and include more low-perfusion vessels (*open arrows*) versus well perfused vessels (*closed arrows*). RBC, red blood cell. Adapted from Reference 7. (*b*) RBC velocity in normal pial vessels versus in brain tumors in mice. Flow rates in normal vessels exhibit a dependency on vessel diameter, whereas tumor vessels demonstrate sluggish flow and a lack of such a correlation. Adapted from Reference 12. (*c*) Properties of brain tumor, peritumoral, and normal blood vessels in the mouse brain. A large fraction of tumor vessels are hypoperfused and feature low hematocrit, whereas normal vessels are well perfused with higher hematocrit. Tumor vessels also demonstrate widely varied diameters and velocities. Reproduced from Reference 7.

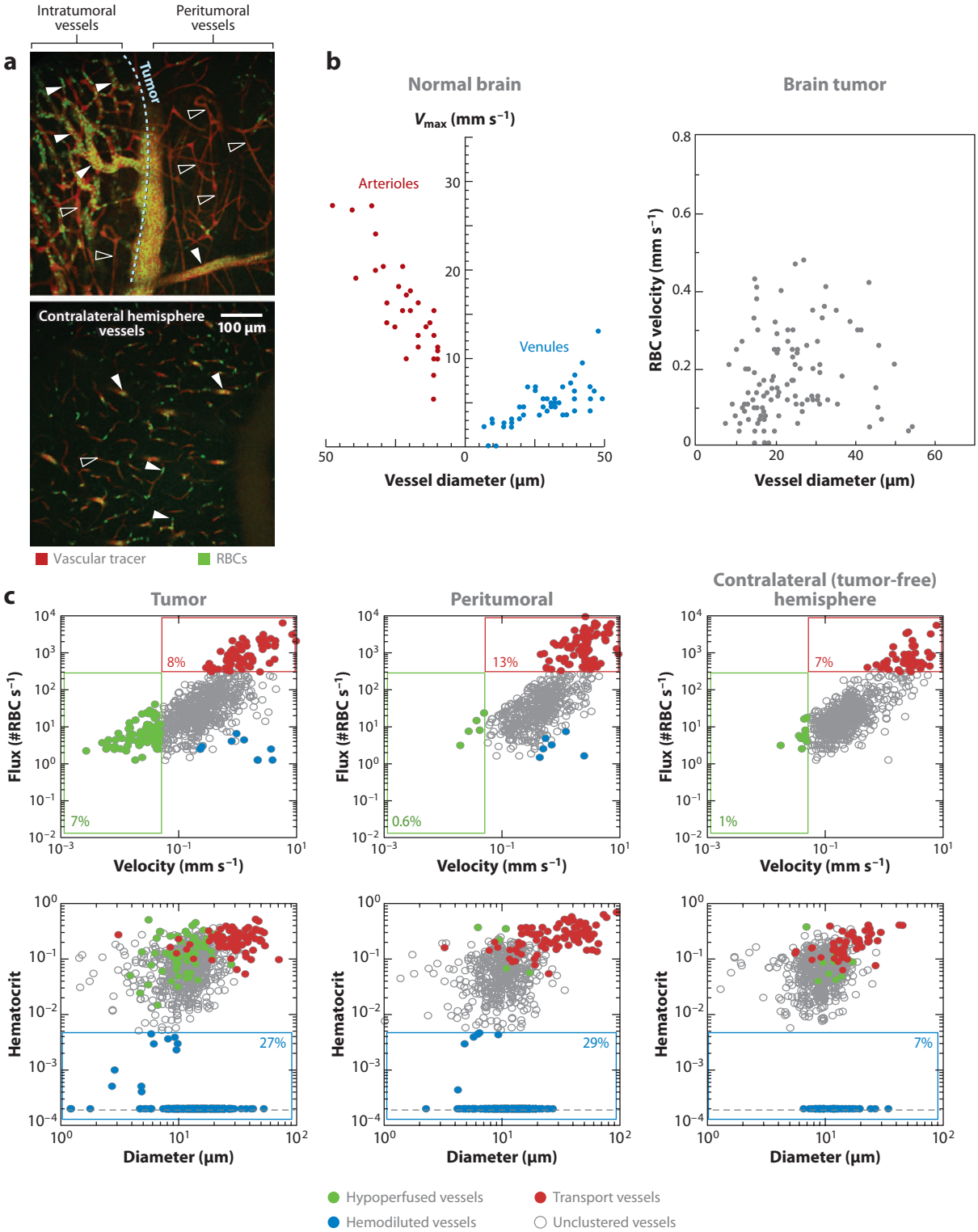

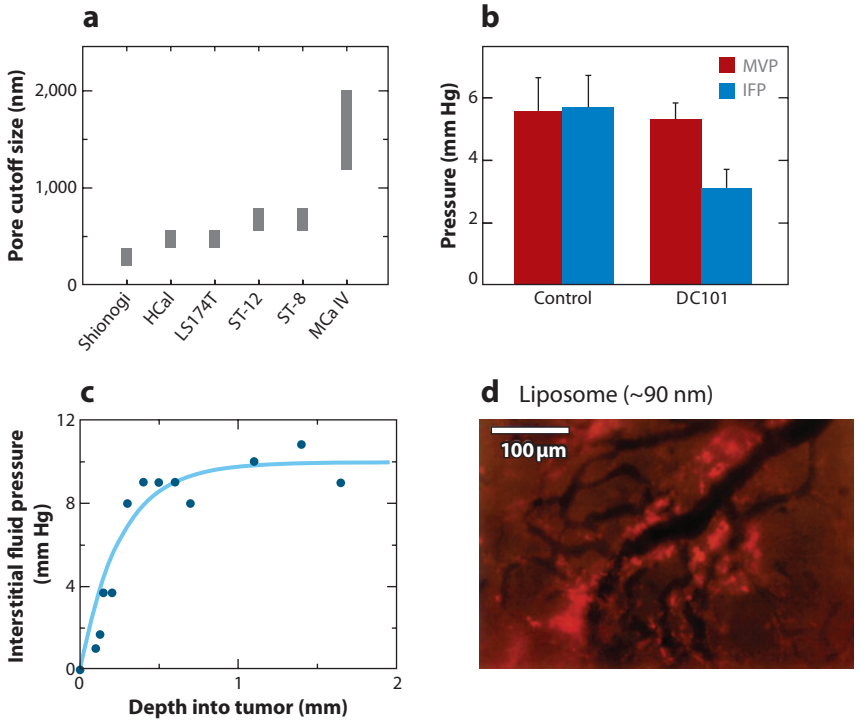

Figure 4

Elevated interstitial fluid pressure (IFP). (*a*) Pore cutoff size, the maximal pore size throughout an entire tumor, in several tumors in mice. Although average pore sizes can be much smaller, these sizes demonstrate how leaky the vasculature can be. Reproduced from Reference 56. (*b*) Microvascular pressure (MVP) and IFP measurements in breast cancers in mice. Both pressures are equal in the control; antiangiogenic therapy with an antibody (DC101) that reduces vessel leakiness decreases IFP while maintaining MVP. Reproduced from Reference 59. (*c*) Interstitial fluid pressure profiles in tumors in rats. Pressure profiles increase sharply at the periphery and then become flat and elevated in the core. Reproduced from Reference 45. (*d*) Tumor penetration of liposomes in a subcutaneous tumor in a mouse. Due to uneven leakiness of vessels and transport solely by diffusion, tumor penetration is heterogeneous. Reproduced from Reference 61.

blood vessel must supply in tumors, this results in short penetration distances and poor drug distribution (61). An additional consequence of the flat fluid pressure profile within tumors and the coupling between microvascular pressure and interstitial fluid pressure is that the pressure drop along the length of intratumoral vessels is diminished (9, 62), further slowing tumor blood flow along with the flow resistance barriers and leading to heterogeneous flow that features stoppages and reversals. In some cases, therapeutics can be convectively driven back into the circulation (33), likely by transient increases in the local interstitial fluid pressure above the microvascular pressure (9). Meanwhile, the vascular pores are generally large compared with those in most normal tissues but are extremely varied in size (56); the vascular basement membrane and associated pericytes are also abnormal in organization (59, 63, 64). These properties compound the blood flow and diffusion-based variabilities in drug distribution to make drug delivery to tumors extremely heterogeneous. Altogether, elevated interstitial fluid pressure hinders vascular, transvascular, and interstitial transport.

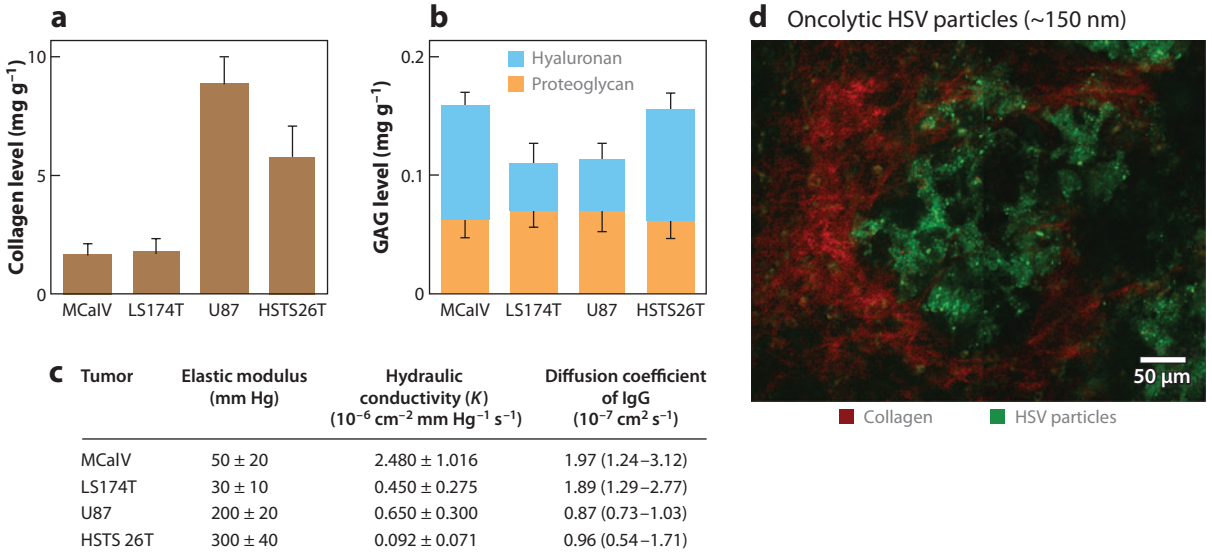

c

Tumor	Elastic modulus (mm Hg)	Hydraulic conductivity (K) (10^{-6} cm^{-2} mm Hg^{-1} s^{-1})	Diffusion coefficient of IgG (10^{-7} cm^{2} s^{-1})
MCaIV	50 ± 20	2.480 ± 1.016	1.97 (1.24–3.12)
LS174T	30 ± 10	0.450 ± 0.275	1.89 (1.29–2.77)
U87	200 ± 20	0.650 ± 0.300	0.87 (0.73–1.03)
HSTS 26T	300 ± 40	0.092 ± 0.071	0.96 (0.54–1.71)

Figure 5

Dense interstitial structure. (*a*) Collagen and (*b*) glycosaminoglycan (GAG) levels in four types of subcutaneous tumors in mice. Both vary greatly from tumor to tumor. Reproduced from Reference 21. (*c*) Transport parameters in the same tumors. Generally, diffusion rates inversely correlate with collagen levels. IgG, immunoglobulin G. Reproduced from Reference 21. (*d*) Oncolytic herpes simplex virus (HSV) particle penetration in a subcutaneous tumor in a mouse. Collagen serves as a steric barrier to virus transport, restricting virus distribution and thus limiting therapeutic effectiveness. Reproduced from Reference 19.

Dense Interstitial Structure

An unusually high stromal fraction in many tumors leads to a desmoplastic state characterized by the formation of fibrous tissue and featuring high levels of interstitial matrix molecules (**Figure 5**) (65, 66). The often high cellularity of tumors, which is largely responsible for the accumulation of solid stress, compresses the matrix into a dense and tortuous network (18). This matrix, which is composed largely of structural molecules such as collagen and space-filling hydrogel-like glycosaminoglycans such as hyaluronan (65, 66), tends to be highly viscoelastic (21). Furthermore, interstitial density generally increases toward the center of a tumor (67), perhaps owing to greater cell density or increased matrix production deeper in the tumor core.

Because the viscosity of the interstitial fluid, the fiber matrix of the interstitium, and the hindrance of large bodies such as cells govern interstitial transport (68, 69), the dense and tortuous tumor interstitium becomes a major barrier for drug delivery. Increasing the size of therapeutics leads to a heightened diffusive hindrance, and free diffusion transitions to anomalous subdiffusion for particles greater than approximately 5–8 nm in diameter (21). Diffusion rates for larger molecules correlate with fibrillar collagen levels (21, 70), organization (71), and orientation (72). Furthermore, fibrillar collagens can serve as a steric barrier to the transport of larger therapeutic agents (19). The contribution of glycosaminoglycans such as hyaluronan to macromolecular diffusion is reversed, with the elimination of hyaluronan decreasing transport, as the interactions between collagen and hyaluronan are quite complex—the two form distinct phases on the micrometer level (18, 35). Meanwhile, the hydraulic conductivity of the interstitium is influenced largely by glycosaminoglycan levels and collagen content; increasing glycosaminoglycan or collagen concentrations lead to increased flow resistance (73, 74). The tortuosity of the interstitial space is an additional barrier for all sizes of drugs or drug carriers because it makes path lengths

for diffusion from blood vessels to target cells extremely long (18). Because many drugs bind to matrix and cellular components, interstitial transport rates become even lower. Additionally, the dense matrix can serve to transmit the solid stress produced by cells to the blood vessels, which enables their compression (5). Thus, the dense interstitium limits both interstitial and vascular transport.

STRATEGIES TO OVERCOME DELIVERY BARRIERS

With general knowledge of the nature of these barriers comes an understanding of the physiological processes that must be modulated to improve drug delivery. Each transport step can be improved by changing the characteristics of the tumor microenvironment. Generally, these approaches involve restoring the abnormal physiology of tumors toward that of normal tissue. As such, we consider each abnormal physiological property of tumors as a target for normalization.

Alleviating Solid Stress

Reducing the accumulated solid stress in tumors may result in an improvement in functional vascular density to increase the supply of drugs to tumors through enhanced vascular transport. By restoring perfusion in regions with compressed vessels, the tumor tissue volume each vessel must supply is reduced, and therefore drug distribution is improved. As a proof of concept, selectively eliminating cancer cells in a human tumor xenograft in a mouse using diphtheria toxin increases the functional vascular density (5). Interestingly, reducing solid stress does not restore function to lymphatic vessels (5); thus, such a strategy would not completely eliminate interstitial hypertension in tumors.

Translatable strategies have been developed that reduce solid stress by targeting these individual components. The killing of cancer cells with taxane therapy improves vessel perfusion by increasing vascular diameters and blood flow rates, likely through reductions in solid stress (2). Combined with a repetitive or metronomic dosing schedule, this could result in improved transport for subsequent doses due to increased supply. Alternatively, the Hedgehog pathway can be targeted using IPI-926, a Hedgehog inhibitor, which reduces the stromal load in pancreatic tumors (75). This leads to improved vascular proliferation and density and thus enhanced delivery, which results in a greater effectiveness for the small-molecule cytotoxic agent gemcitabine. Importantly, these strategies are fully compatible as part of combination therapy because they target different pathways.

Normalizing Vascular Network Function

Enhancing the efficiency of the tumor vascular network by increasing blood flow to tumors or improving vessel organization will enhance drug delivery for most sizes of drug molecules by improving blood supply. Tumor blood flow can be improved by changes to the arterial blood pressure or to blood viscosity itself, though such systemic changes generally are not selective versus normal tissue blood flow (76). For specific improvements in tumor blood flow, targeting the tumor microenvironment to reduce the geometric or viscous resistance is necessary. For example, reducing vascular permeability in tumors may improve flow by preventing hemoconcentration, as indicated by improvements in tumor oxygenation with such a change (77–79). However, it is not clear if permeability changes alone will have a significant effect, as most studies involve multiple modifications to tumor vasculature. Reductions in vascular tortuosity and branching

are also expected to improve blood flow, though the independent effects of alterations to these geometric resistance factors have not been clarified.

The few approaches to improving vascular network function are not necessarily appealing as translatable therapies. The most successful have focused on reducing viscous resistance by modulating blood properties. Hemodilution reduces viscous resistance to selectively improve mean tumor blood flow (80), but such an approach alone is unlikely to be appropriate in the clinic. Pentoxifylline improves average tumor blood flow selectively, likely through a rheological effect on blood cells (81). Unfortunately, there are no proven pharmacological mechanisms for improving flow into tumors by repairing the vessel network structure itself. Furthermore, it is unclear if changes in vascular permeability will have a great effect on average blood flow unless the entire vessel network of a tumor is repaired, as interstitial fluid pressure seems to have little correlation with oxygenation in unmodified tumors (82). Several changes to the tumor microenvironment likely must be induced to significantly improve flow, including correction of solid stress and interstitial hypertension along with changes in vascular tortuosity. Still, all considered approaches remain in the theoretical or proof-of-principle stage, and thus there is currently no translatable means of improving mean blood flow in tumors. However, it is more important to make blood perfusion rates more uniform than to improve average blood flow; the former can be achieved by lowering vascular permeability with antiangiogenic agents to reduce interstitial fluid pressure (52, 83, 84).

Reducing Interstitial Hypertension

Because the elevated interstitial fluid pressure in tumors hinders both vascular and transvascular transport, it is a major target for improving drug delivery. Uncoupling tumor interstitial fluid pressure from the microvascular pressure can restore local transmural pressure gradients to drive faster transvascular transport and improve perfusion rates. A great deal of evidence exists to support this hypothesis. Exploiting the brief delay in interstitial fluid pressure tracking of microvascular pressure by brief pulsed infusions that create a transient transmural pressure gradient results in improved transvascular transport of fluid and macromolecular agents (85). Improving interstitial hydraulic conductivity can reduce interstitial fluid pressure by allowing for faster peritumoral fluid clearance. Collagenase-induced reductions in interstitial fluid pressure can restore convective mass transport for antibody probes (86). Similarly, hyaluronidase-induced restoration of a transmural pressure gradient improves transvascular transport of nanoprobes (87).

Modulating transvascular transport by reducing interstitial fluid pressure has been explored a great deal; one strategy has been implemented in the clinic. Anti-angiogenic therapies, for example those targeting the VEGF pathway, induce vessel normalization in tumors, leading to pruning of unnecessary immature vessels, reductions in vessel diameter, improvements in perfusion, and decreases in vessel tortuosity (59, 79). The resulting normalized vessels feature reduced vessel wall pore sizes, which lead to a drop in interstitial fluid pressure and restoration of transvascular pressure gradients (59, 79). These changes to vascular function and the restoration of a transmural pressure gradient result in improved delivery of therapeutic agents and oxygen (59, 88, 89). Anti-VEGF therapy improves transport for small agents, although the decreased pore sizes may represent a steric barrier for larger nanoparticles that could counteract the enhancement in convective transvascular transport. Anti-angiogenic therapy with the anti-VEGF agent bevacizumab leads to reduced interstitial fluid pressure, decreased vascular density, and improved tracer delivery in patients with colorectal cancer (90). Similarly, the anti-VEGF-receptor agent cediranib reduces vascular permeability, vessel size, and edema in patients with recurrent glioblastoma (91). A challenge for this approach to improving drug delivery is the identification of alternative pathways to target when tumors become resistant to therapies targeting the VEGF pathway.

Diminishing Interstitial Density

For nanomedicine in particular, modulating the levels of tumor interstitium constituents can result in improved interstitial transport, leading to enhanced drug distribution and effectiveness. Degradation of collagen with bacterial collagenase can double diffusion rates for immunoglobulin G antibodies and other probes (21, 35, 67). This improvement in transport corresponds to approximately a threefold improvement in oncolytic herpes simplex virus distribution, which is associated with a significant improvement in virus effectiveness in tumor models (19, 92). Ectopic expression of matrix metalloproteinases-1 and -8 in tumor cells decreases sulfated glycosaminoglycan content in implanted tumors to enhance interstitial hydraulic conductivity (20). Similarly, degradation of the glycosaminoglycan hyaluronan with hyaluronidase improves hydraulic conductivity in tissues (93) while decreasing diffusion of nanosized probes (35, 94). Combined with reductions in interstitial fluid pressure, such changes in hydraulic conductivity may improve systemic drug delivery. Finally, eliminating cells from a tumor can increase the interstitial transport and distribution of nanotherapeutics by decreasing the tortuosity of the interstitium (18, 95).

A few translatable approaches for improving interstitial transport have come about recently. Relaxin, a hormone produced during pregnancy, modulates collagen fiber structure to improve diffusion of nanosized probes two- to threefold (71, 96). However, perhaps due to its mechanism as a matrix-degrading therapy, there are some indications that relaxin may lead to increased metastasis. Recombinant human hyaluronidase can improve convective transport of agents following local injection (97). However, such a strategy will likely require additional therapies to improve systemic delivery of therapeutics because it may not restore a transvascular pressure gradient. The FDA-approved antihypertensive agent losartan, through inhibition of TGF-β and CTGF activity, prevents matrix production in tumors (98). The resulting reduction in collagen content improves diffusion for antibody probes 1.5-fold, resulting in enhanced herpes simplex virus and nanoparticle distribution in tumors with corresponding increases in effectiveness for the virus or the nanoparticle doxil in tumor models. Again, all these strategies are compatible due to their different targets and kinetics; thus, they could be candidates for combination approaches to adjunct therapy.

Tuning Therapeutic Agent Properties

A great deal of effort has been put into the development of design rules for drugs and nanoparticles. Physical properties of drugs or drug vehicles, including their size, charge, and configuration, affect all three types of transport processes in tumors.

Size is perhaps the best-studied property in relation to drug transport. Agents smaller than 5–6 nm or 30–50 kDa can undergo rapid renal clearance due to passage through glomerular pores (99, 100), but increasing size in the nanometer range also results in greater hepatobiliary and reticuloendothelial clearance (101). As such, the optimal agent for vascular transport must avoid the <5–6 nm regime while remaining as small as possible in the nanometer size range. Generally, larger nanometer-sized particles are greatly hindered in transvascular transport (101, 102) because much variability exists in tumor vascular pore sizes; only small fractions of pores are in the hundreds of nanometers size range (55, 56). In most tissues, interstitial transport of particles larger than a few tens of nanometers is greatly hindered, perhaps as an evolved mechanism for resistance to viral and bacterial infection, as these pathogens range from tens of nanometers to micrometers in size. In tumor interstitium, particles larger than 5–8 nm experience hindered diffusion; rates are slowed by up to two orders of magnitude for 40-nm particles (22). Furthermore, particles of increasing size generally experience increasing hindrance versus solution diffusion rates (103). Overall, small or size-changing agents are ideal for optimal drug delivery efficiency (104).

Surface charge plays a complex role in the transport of therapeutic agents. Clearance rates depend highly on surface properties (105, 106). Interactions with the reticuloendothelial system, and thus clearance rates, tend to increase with charge. Surface modification with poly(ethylene glycol) or similar polymers can neutralize particles, which prevents opsonization by serum proteins and uptake by Kupffer cells or hepatocytes (107–109). Meanwhile, cationic nanoparticles can bind to endothelial cells, which results in faster transvascular transport versus neutral or anionic particles (110–114). Neutral nanoparticles also display the fastest interstitial transport because charged particles are limited by binding or volume-excluding interactions with negatively charged glycosaminoglycans or positively charged collagens (115, 116). Such charge-charge interactions can aggregate charged agents, hindering transport by up to three orders of magnitude (20, 21, 115, 117, 118). Thus neutral agents, or perhaps agents that change charge or have zwitterionic character, may exhibit the best transport to tumors.

Shape and rigidity perhaps have been the least-studied properties affecting therapeutic agent transport. Flexible rods have longer half-lives than do rigid rods, possibly owing to a unique alignment to flow streamlines that prevents phagocytosis (119). The kidneys can rapidly clear thin rods with a shorter dimension smaller than the 5–6 nm filtration cutoff of glomerular membranes; alignment to flow strongly increases the probability of passage through the pores (120). During in vitro agarose diffusion studies, flexible nanometer-sized rods exhibit greater mobilities than do rigid rods or spheres of similar hydrodynamic diameter due to reptation (121), although it is unclear if this will hold true in the more complex tumor interstitium. Altogether, it appears that flexible, nanometer-range particles demonstrate ideal transport properties, but additional studies are necessary for optimization of aspect ratios.

CONCLUSION

The treatment of cancer, as a disseminated disease, requires therapeutics that are capable of efficiently navigating their way through a series of transport steps. Physiological abnormalities lead to barriers to these steps that hinder delivery; together they compose a mechanical resistance mechanism to cancer therapeutics. To overcome these barriers, these abnormal physiological states need to be repaired toward normalcy. Additionally, the physicochemical properties of therapeutic agents must be optimized for efficient delivery. Based on a quantitative understanding of tumors as systems, these and other strategies can be developed in concert with novel drug and drug carrier development. The rational design of combinations against the tumor microenvironment as well as tumor cells may bring hope for highly effective therapies.

DISCLOSURE STATEMENT

R.K. Jain has received consulting fees from Astellas, AstraZeneca, Dyax, Enlight Biosciences, Genzyme, Noxxon, and SynDevRx; lecture fees from Genzyme and MPM Capital; and grant support from Dyax, MedImmune, and Roche. He also owns equity in Enlight Biosciences and SynDevRx.

ACKNOWLEDGMENTS

We thank Benjamin Diop-Frimpong and John D. Martin for helpful comments. This review is based on the following previous review article: Jain, R. K. Delivery of molecular and cellular medicine to solid tumors (1). This work was supported by the National Institutes of Health (PO1-CA80124, RO1-CA126642, RO1-CA115767, RO1-CA85140, R01-CA98706, T32-CA73479),

Federal Share Income Grant, and DoD Breast Cancer Research Innovator award (W81XWH-10-1-0016). T.S. was supported by a postdoctoral research fellowship from the Susan G. Komen Breast Cancer Foundation (KG091281).

LITERATURE CITED

1. Jain RK. 2001. Delivery of molecular and cellular medicine to solid tumors. *Adv. Drug Deliv. Rev.* 46:149–68
2. Griffon-Etienne G, Boucher Y, Brekken C, Suit HD, Jain RK. 1999. Taxane-induced apoptosis decompresses blood vessels and lowers interstitial fluid pressure in solid tumors: clinical implications. *Cancer Res.* 59:3776–82
3. Helmlinger G, Netti PA, Lichtenbeld HC, Melder RJ, Jain RK. 1997. Solid stress inhibits the growth of multicellular tumor spheroids. *Nat. Biotechnol.* 15:778–83
4. Leu AJ, Berk DA, Lymboussaki A, Alitalo K, Jain RK. 2000. Absence of functional lymphatics within a murine sarcoma: a molecular and functional evaluation. *Cancer Res.* 60:4324–27
5. Padera TP, Stoll BR, Tooredman JB, Capen D, di Tomaso E, Jain RK. 2004. Pathology: cancer cells compress intratumour vessels. *Nature* 427:695
6. Gazit Y, Berk DA, Leunig M, Baxter LT, Jain RK. 1995. Scale-invariant behavior and vascular network formation in normal and tumor tissue. *Phys. Rev. Lett.* 75:2428–31
7. Kamoun WS, Chae SS, Lacorre DA, Tyrrell JA, Mitre M, et al. 2010. Simultaneous measurement of RBC velocity, flux, hematocrit and shear rate in vascular networks. *Nat. Methods* 7:655–60
8. Leunig M, Yuan F, Menger MD, Boucher Y, Goetz AE, et al. 1992. Angiogenesis, microvascular architecture, microhemodynamics, and interstitial fluid pressure during early growth of human adenocarcinoma LS174T in SCID mice. *Cancer Res.* 52:6553–60
9. Netti PA, Roberge S, Boucher Y, Baxter LT, Jain RK. 1996. Effect of transvascular fluid exchange on pressure-flow relationship in tumors: a proposed mechanism for tumor blood flow heterogeneity. *Microvasc. Res.* 52:27–46
10. Sevick EM, Jain RK. 1989. Viscous resistance to blood flow in solid tumors: effect of hematocrit on intratumor blood viscosity. *Cancer Res.* 49:3513–19
11. Sevick EM, Jain RK. 1989. Geometric resistance to blood flow in solid tumors perfused ex vivo: effects of tumor size and perfusion pressure. *Cancer Res.* 49:3506–12
12. Yuan F, Salehi HA, Boucher Y, Vasthare US, Tuma RF, Jain RK. 1994. Vascular permeability and microcirculation of gliomas and mammary carcinomas transplanted in rat and mouse cranial windows. *Cancer Res.* 54:4564–68
13. Baish JW, Stylianopoulos T, Lanning RM, Kamoun WS, Fukumura D, et al. 2011. Scaling rules for diffusive drug delivery in tumor and normal tissues. *Proc. Natl. Acad. Sci. USA* 108:1799–803
14. Boucher Y, Jain RK. 1992. Microvascular pressure is the principal driving force for interstitial hypertension in solid tumors: implications for vascular collapse. *Cancer Res.* 52:5110–14
15. Jain RK. 1994. Barriers to drug delivery in solid tumors. *Sci. Am.* 271:58–65
16. Jain RK, Tong RT, Munn LL. 2007. Effect of vascular normalization by antiangiogenic therapy on interstitial hypertension, peritumor edema, and lymphatic metastasis: insights from a mathematical model. *Cancer Res.* 67:2729–35
17. Netti PA, Baxter LT, Boucher Y, Skalak R, Jain RK. 1995. Time-dependent behavior of interstitial fluid pressure in solid tumors: implications for drug delivery. *Cancer Res.* 55:5451–58
18. Chauhan VP, Lanning RM, Diop-Frimpong B, Mok W, Brown EB, et al. 2009. Multiscale measurements distinguish cellular and interstitial hindrances to diffusion in vivo. *Biophys. J.* 97:330–36
19. McKee TD, Grandi P, Mok W, Alexandrakis G, Insin N, et al. 2006. Degradation of fibrillar collagen in a human melanoma xenograft improves the efficacy of an oncolytic herpes simplex virus vector. *Cancer Res.* 66:2509–13
20. Mok W, Boucher Y, Jain RK. 2007. Matrix metalloproteinases-1 and -8 improve the distribution and efficacy of an oncolytic virus. *Cancer Res.* 67:10664–68

21. Netti PA, Berk DA, Swartz MA, Grodzinsky AJ, Jain RK. 2000. Role of extracellular matrix assembly in interstitial transport in solid tumors. *Cancer Res.* 60:2497–503
22. Pluen A, Boucher Y, Ramanujan S, McKee TD, Gohongi T, et al. 2001. Role of tumor-host interactions in interstitial diffusion of macromolecules: cranial versus subcutaneous tumors. *Proc. Natl. Acad. Sci. USA* 98:4628–33
23. Harris AL. 2002. Hypoxia—a key regulatory factor in tumour growth. *Nat. Rev.* 2:38–47
24. Minchinton AI, Tannock IF. 2006. Drug penetration in solid tumours. *Nat. Rev.* 6:583–92
25. Flessner MF. 2005. The transport barrier in intraperitoneal therapy. *Am. J. Physiol. Renal Physiol.* 288:F433–42
26. Jain RK, Stylianopoulos T. 2010. Delivering nanomedicine to solid tumors. *Nat. Rev.* 7:653–64
27. Brown EB, Campbell RB, Tsuzuki Y, Xu L, Carmeliet P, et al. 2001. In vivo measurement of gene expression, angiogenesis and physiological function in tumors using multiphoton laser scanning microscopy. *Nat. Med.* 7:864–68
28. Vakoc BJ, Lanning RM, Tyrrell JA, Padera TP, Bartlett LA, et al. 2009. Three-dimensional microscopy of the tumor microenvironment in vivo using optical frequency domain imaging. *Nat. Med.* 15:1219–23
29. Gerlowski LE, Jain RK. 1986. Microvascular permeability of normal and neoplastic tissues. *Microvasc. Res.* 31:288–305
30. Yuan F, Leunig M, Berk DA, Jain RK. 1993. Microvascular permeability of albumin, vascular surface area, and vascular volume measured in human adenocarcinoma LS174T using dorsal chamber in SCID mice. *Microvasc. Res.* 45:269–89
31. Axelrod D, Koppel DE, Schlessinger J, Elson E, Webb WW. 1976. Mobility measurement by analysis of fluorescence photobleaching recovery kinetics. *Biophys. J.* 16:1055–69
32. Berk DA, Yuan F, Leunig M, Jain RK. 1993. Fluorescence photobleaching with spatial Fourier analysis: measurement of diffusion in light-scattering media. *Biophys. J.* 65:2428–36
33. Chary SR, Jain RK. 1989. Direct measurement of interstitial convection and diffusion of albumin in normal and neoplastic tissues by fluorescence photobleaching. *Proc. Natl. Acad. Sci. USA* 86:5385–89
34. Magde D, Webb WW, Elson E. 1972. Thermodynamic fluctuations in a reacting system—measurement by fluorescence correlation spectroscopy. *Phys. Rev. Lett.* 29:705–8
35. Alexandrakis G, Brown EB, Tong RT, McKee TD, Campbell RB, et al. 2004. Two-photon fluorescence correlation microscopy reveals the two-phase nature of transport in tumors. *Nat. Med.* 10:203–7
36. Berland KM, So PT, Gratton E. 1995. Two-photon fluorescence correlation spectroscopy: method and application to the intracellular environment. *Biophys. J.* 68:694–701
37. Brown EB, Wu ES, Zipfel W, Webb WW. 1999. Measurement of molecular diffusion in solution by multiphoton fluorescence photobleaching recovery. *Biophys. J.* 77:2837–49
38. Cheng G, Tse J, Jain RK, Munn LL. 2009. Micro-environmental mechanical stress controls tumor spheroid size and morphology by suppressing proliferation and inducing apoptosis in cancer cells. *PLoS ONE* 4:e4632
39. Koike C, McKee TD, Pluen A, Ramanujan S, Burton K, et al. 2002. Solid stress facilitates spheroid formation: potential involvement of hyaluronan. *Br. J. Cancer* 86:947–53
40. Jain RK. 1988. Determinants of tumor blood flow: a review. *Cancer Res.* 48:2641–58
41. Baish JW, Gazit Y, Berk DA, Nozue M, Baxter LT, Jain RK. 1996. Role of tumor vascular architecture in nutrient and drug delivery: an invasion percolation-based network model. *Microvasc. Res.* 51:327–46
42. Endrich B, Reinhold HS, Gross JF, Intaglietta M. 1979. Tissue perfusion inhomogeneity during early tumor growth in rats. *J. Natl. Cancer Inst.* 62:387–95
43. Helmlinger G, Yuan F, Dellian M, Jain RK. 1997. Interstitial pH and pO_2 gradients in solid tumors in vivo: high-resolution measurements reveal a lack of correlation. *Nat. Med.* 3:177–82
44. Young JS, Lumsden CE, Stalker AL. 1950. The significance of the tissue pressure of normal testicular and of neoplastic (Brown-Pearce carcinoma) tissue in the rabbit. *J. Pathol. Bacteriol.* 62:313–33
45. Boucher Y, Baxter LT, Jain RK. 1990. Interstitial pressure gradients in tissue-isolated and subcutaneous tumors: implications for therapy. *Cancer Res.* 50:4478–84
46. Jain RK, Baxter LT. 1988. Mechanisms of heterogeneous distribution of monoclonal antibodies and other macromolecules in tumors: significance of elevated interstitial pressure. *Cancer Res.* 48:7022–32

47. Carmeliet P, Jain RK. 2000. Angiogenesis in cancer and other diseases. *Nature* 407:249–57
48. Gimbrone MA Jr, Leapman SB, Cotran RS, Folkman J. 1972. Tumor dormancy in vivo by prevention of neovascularization. *J. Exp. Med.* 136:261–76
49. Folkman J, Hochberg M. 1973. Self-regulation of growth in three dimensions. *J. Exp. Med.* 138:745–53
50. Knighton D, Ausprunk D, Tapper D, Folkman J. 1977. Avascular and vascular phases of tumour growth in the chick embryo. *Br. J. Cancer* 35:347–56
51. Hanahan D, Weinberg RA. 2000. The hallmarks of cancer. *Cell* 100:57–70
52. Jain RK. 2003. Molecular regulation of vessel maturation. *Nat. Med.* 9:685–93
53. Nagy JA, Dvorak AM, Dvorak HF. 2007. VEGF-A and the induction of pathological angiogenesis. *Annu. Rev. Pathol. Mech. Dis.* 2:251–75
54. Dvorak HF, Brown LF, Detmar M, Dvorak AM. 1995. Vascular permeability factor/vascular endothelial growth factor, microvascular hyperpermeability, and angiogenesis. *Am. J. Pathol.* 146:1029–39
55. Hashizume H, Baluk P, Morikawa S, McLean JW, Thurston G, et al. 2000. Openings between defective endothelial cells explain tumor vessel leakiness. *Am. J. Pathol.* 156:1363–80
56. Hobbs SK, Monsky WL, Yuan F, Roberts WG, Griffith L, et al. 1998. Regulation of transport pathways in tumor vessels: role of tumor type and microenvironment. *Proc. Natl. Acad. Sci. USA* 95:4607–12
57. Roberts WG, Palade GE. 1997. Neovasculature induced by vascular endothelial growth factor is fenestrated. *Cancer Res.* 57:765–72
58. Sun C, Jain RK, Munn LL. 2007. Non-uniform plasma leakage affects local hematocrit and blood flow: implications for inflammation and tumor perfusion. *Ann. Biomed. Eng.* 35:2121–29
59. Tong RT, Boucher Y, Kozin SV, Winkler F, Hicklin DJ, Jain RK. 2004. Vascular normalization by vascular endothelial growth factor receptor 2 blockade induces a pressure gradient across the vasculature and improves drug penetration in tumors. *Cancer Res.* 64:3731–36
60. Padera TP, Kadambi A, di Tomaso E, Carreira CM, Brown EB, et al. 2002. Lymphatic metastasis in the absence of functional intratumor lymphatics. *Science* 296:1883–86
61. Yuan F, Leunig M, Huang SK, Berk DA, Papahadjopoulos D, Jain RK. 1994. Microvascular permeability and interstitial penetration of sterically stabilized (stealth) liposomes in a human tumor xenograft. *Cancer Res.* 54:3352–56
62. Baish JW, Netti PA, Jain RK. 1997. Transmural coupling of fluid flow in microcirculatory network and interstitium in tumors. *Microvasc. Res.* 53:128–41
63. Kalluri R. 2003. Basement membranes: structure, assembly and role in tumour angiogenesis. *Nat. Rev.* 3:422–33
64. Nyberg P, Salo T, Kalluri R. 2008. Tumor microenvironment and angiogenesis. *Front. Biosci.* 13:6537–53
65. Dvorak HF. 1986. Tumors: wounds that do not heal. Similarities between tumor stroma generation and wound healing. *N. Engl. J. Med.* 315:1650–59
66. Ronnov-Jessen L, Petersen OW, Bissell MJ. 1996. Cellular changes involved in conversion of normal to malignant breast: importance of the stromal reaction. *Physiol. Rev.* 76:69–125
67. Magzoub M, Jin S, Verkman AS. 2008. Enhanced macromolecule diffusion deep in tumors after enzymatic digestion of extracellular matrix collagen and its associated proteoglycan decorin. *FASEB J.* 22:276–84
68. Nandigam RK, Kroll DM. 2007. Three-dimensional modeling of the brain's ECS by minimum configurational energy packing of fluid vesicles. *Biophys. J.* 92:3368–78
69. Piet R, Vargova L, Sykova E, Poulain DA, Oliet SH. 2004. Physiological contribution of the astrocytic environment of neurons to intersynaptic crosstalk. *Proc. Natl. Acad. Sci. USA* 101:2151–55
70. Ramanujan S, Pluen A, McKee TD, Brown EB, Boucher Y, Jain RK. 2002. Diffusion and convection in collagen gels: implications for transport in the tumor interstitium. *Biophys. J.* 83:1650–60
71. Brown E, McKee T, diTomaso E, Pluen A, Seed B, et al. 2003. Dynamic imaging of collagen and its modulation in tumors in vivo using second-harmonic generation. *Nat. Med.* 9:796–800
72. Stylianopoulos T, Diop-Frimpong B, Munn LL, Jain RK. 2010. Diffusion anisotropy in collagen gels and tumors: the effect of fiber network orientation. *Biophys. J.* 99:3119–28
73. Ogston AG, Sherman TF. 1961. Effects of hyaluronic acid upon diffusion of solutes and flow of solvent. *J. Physiol.* 156:67–74

74. Znati CA, Rosenstein M, McKee TD, Brown E, Turner D, et al. 2003. Irradiation reduces interstitial fluid transport and increases the collagen content in tumors. *Clin. Cancer Res.* 9:5508–13
75. Olive KP, Jacobetz MA, Davidson CJ, Gopinathan A, McIntyre D, et al. 2009. Inhibition of Hedgehog signaling enhances delivery of chemotherapy in a mouse model of pancreatic cancer. *Science* 324:1457–61
76. Zlotecki RA, Baxter LT, Boucher Y, Jain RK. 1995. Pharmacologic modification of tumor blood flow and interstitial fluid pressure in a human tumor xenograft: network analysis and mechanistic interpretation. *Microvasc. Res.* 50:429–43
77. Kashiwagi S, Tsukada K, Xu L, Miyazaki J, Kozin SV, et al. 2008. Perivascular nitric oxide gradients normalize tumor vasculature. *Nat. Med.* 14:255–57
78. Mazzone M, Dettori D, Leite de Oliveira R, Loges S, Schmidt T, et al. 2009. Heterozygous deficiency of *PHD2* restores tumor oxygenation and inhibits metastasis via endothelial normalization. *Cell* 136:839–51
79. Winkler F, Kozin SV, Tong RT, Chae SS, Booth MF, et al. 2004. Kinetics of vascular normalization by VEGFR2 blockade governs brain tumor response to radiation: role of oxygenation, angiopoietin-1, and matrix metalloproteinases. *Cancer Cell* 6:553–63
80. Lee I, Demhartner TJ, Boucher Y, Jain RK, Intaglietta M. 1994. Effect of hemodilution and resuscitation on tumor interstitial fluid pressure, blood flow, and oxygenation. *Microvasc. Res.* 48:1–12
81. Lee I, Boucher Y, Demhartner TJ, Jain RK. 1994. Changes in tumor blood flow, oxygenation and interstitial fluid pressure induced by pentoxifylline. *Br. J. Cancer* 69:492–96
82. Boucher Y, Lee I, Jain RK. 1995. Lack of general correlation between interstitial fluid pressure and oxygen partial pressure in solid tumors. *Microvasc. Res.* 50:175–82
83. Jain RK. 2005. Normalization of tumor vasculature: an emerging concept in antiangiogenic therapy. *Science* 307:58–62
84. Jain RK. 2008. Taming vessels to treat cancer. *Sci. Am.* 298:56–63
85. Netti PA, Hamberg LM, Babich JW, Kierstead D, Graham W, et al. 1999. Enhancement of fluid filtration across tumor vessels: implication for delivery of macromolecules. *Proc. Natl. Acad. Sci. USA* 96:3137–42
86. Eikenes L, Bruland ØS, Brekken C, de Lange Davies C. 2004. Collagenase increases the transcapillary pressure gradient and improves the uptake and distribution of monoclonal antibodies in human osteosarcoma xenografts. *Cancer Res.* 64:4768–73
87. Eikenes L, Tari M, Tufto I, Bruland ØS, de Lange Davies C. 2005. Hyaluronidase induces a transcapillary pressure gradient and improves the distribution and uptake of liposomal doxorubicin (Caelyx) in human osteosarcoma xenografts. *Br. J. Cancer* 93:81–88
88. Wildiers H, Guetens G, De Boeck G, Verbeken E, Landuyt B, et al. 2003. Effect of antivascular endothelial growth factor treatment on the intratumoral uptake of CPT-11. *Br. J. Cancer* 88:1979–86
89. Lee CG, Heijn M, di Tomaso E, Griffon-Etienne G, Ancukiewicz M, et al. 2000. Anti-vascular endothelial growth factor treatment augments tumor radiation response under normoxic or hypoxic conditions. *Cancer Res.* 60:5565–70
90. Willett CG, Boucher Y, di Tomaso E, Duda DG, Munn LL, et al. 2004. Direct evidence that the VEGF-specific antibody bevacizumab has antivascular effects in human rectal cancer. *Nat. Med.* 10:145–47
91. Batchelor TT, Sorensen AG, di Tomaso E, Zhang WT, Duda DG, et al. 2007. AZD2171, a pan-VEGF receptor tyrosine kinase inhibitor, normalizes tumor vasculature and alleviates edema in glioblastoma patients. *Cancer Cell* 11:83–95
92. Mok W, Stylianopoulos T, Boucher Y, Jain RK. 2009. Mathematical modeling of herpes simplex virus distribution in solid tumors: implications for cancer gene therapy. *Clin. Cancer Res.* 15:2352–60
93. Lai-Fook SJ, Rochester NL, Brown LV. 1989. Effects of albumin, dextran, and hyaluronidase on pulmonary interstitial conductivity. *J. Appl. Physiol.* 67:606–13
94. Qiu XL, Brown LV, Parameswaran S, Marek VW, Ibbott GS, Lai-Fook SJ. 1999. Effect of hyaluronidase on albumin diffusion in lung interstitium. *Lung* 177:273–88
95. Nagano S, Perentes JY, Jain RK, Boucher Y. 2008. Cancer cell death enhances the penetration and efficacy of oncolytic herpes simplex virus in tumors. *Cancer Res.* 68:3795–802
96. Perentes JY, McKee TD, Ley CD, Mathiew H, Dawson M, et al. 2009. In vivo imaging of extracellular matrix remodeling by tumor-associated fibroblasts. *Nat. Methods* 6:143–45
97. Bookbinder LH, Hofer A, Haller MF, Zepeda ML, Keller GA, et al. 2006. A recombinant human enzyme for enhanced interstitial transport of therapeutics. *J. Control. Release* 114:230–41

98. Diop-Frimpong B, Chauhan VP, Krane S, Boucher Y, Jain RK. 2011. Losartan inhibits collagen I synthesis to improve the distribution and efficacy of nanotherapeutics in tumors. *Proc. Natl. Acad. Sci. USA* 108:2909–14
99. Choi HS, Liu W, Liu F, Nasr K, Misra P, et al. 2010. Design considerations for tumour-targeted nanoparticles. *Nat. Nanotechnol.* 5:42–47
100. Choi HS, Liu W, Misra P, Tanaka E, Zimmer JP, et al. 2007. Renal clearance of quantum dots. *Nat. Biotechnol.* 25:1165–70
101. Popović Z, Liu WH, Chauhan VP, Lee J, Wong C, et al. 2010. A nanoparticle size series for in vivo fluorescence imaging. *Angew. Chem. Int. Ed.* 49:8649–52
102. Yuan F, Dellian M, Fukumura D, Leunig M, Berk DA, et al. 1995. Vascular permeability in a human tumor xenograft: molecular size dependence and cutoff size. *Cancer Res.* 55:3752–56
103. Nugent LJ, Jain RK. 1984. Extravascular diffusion in normal and neoplastic tissues. *Cancer Res.* 44:238–44
104. Wong CR, Stylianopoulos T, Cui J, Martin JD, Chauhan VP, et al. 2011. Multistage nanoparticle delivery system for deep penetration into tumor tissue. *Proc. Natl. Acad. Sci. USA* 108:2426–31
105. Longmire M, Choyke PL, Kobayashi H. 2008. Clearance properties of nano-sized particles and molecules as imaging agents: considerations and caveats. *Nanomedicine* (*Lond.*) 3:703–17
106. Franzen S, Lommel SA. 2009. Targeting cancer with "smart bombs": equipping plant virus nanoparticles for a "seek and destroy" mission. *Nanomedicine* (*Lond.*) 4:575–88
107. Klibanov AL, Maruyama K, Torchilin VP, Huang L. 1990. Amphipathic polyethyleneglycols effectively prolong the circulation time of liposomes. *FEBS Lett.* 268:235–37
108. Peracchia MT, Fattal E, Desmaele D, Besnard M, Noel JP, et al. 1999. Stealth PEGylated polycyanoacrylate nanoparticles for intravenous administration and splenic targeting. *J. Control. Release* 60:121–28
109. Storm G, Belliot SO, Daemen T, Lasic DD. 1995. Surface modification of nanoparticles to oppose uptake by the mononuclear phagocyte system. *Adv. Drug Deliv. Rev.* 17:31–48
110. Campbell RB, Fukumura D, Brown EB, Mazzola LM, Izumi Y, et al. 2002. Cationic charge determines the distribution of liposomes between the vascular and extravascular compartments of tumors. *Cancer Res.* 62:6831–36
111. Schmitt-Sody M, Strieth S, Krasnici S, Sauer B, Schulze B, et al. 2003. Neovascular targeting therapy: paclitaxel encapsulated in cationic liposomes improves antitumoral efficacy. *Clin. Cancer Res.* 9:2335–41
112. Dellian M, Yuan F, Trubetskoy VS, Torchilin VP, Jain RK. 2000. Vascular permeability in a human tumour xenograft: molecular charge dependence. *Br. J. Cancer* 82:1513–18
113. Thurston G, McLean JW, Rizen M, Baluk P, Haskell A, et al. 1998. Cationic liposomes target angiogenic endothelial cells in tumors and chronic inflammation in mice. *J. Clin. Investig.* 101:1401–13
114. Krasnici S, Werner A, Eichhorn ME, Schmitt-Sody M, Pahernik SA, et al. 2003. Effect of the surface charge of liposomes on their uptake by angiogenic tumor vessels. *Int. J. Cancer* 105:561–67
115. Lieleg O, Baumgartel RM, Bausch AR. 2009. Selective filtering of particles by the extracellular matrix: an electrostatic bandpass. *Biophys. J.* 97:1569–77
116. Stylianopoulos T, Poh MZ, Insin N, Bawendi MG, Fukumura D, et al. 2010. Diffusion of particles in the extracellular matrix: the effect of repulsive electrostatic interactions. *Biophys. J.* 99:1342–49
117. Thorne RG, Lakkaraju A, Rodriguez-Boulan E, Nicholson C. 2008. In vivo diffusion of lactoferrin in brain extracellular space is regulated by interactions with heparan sulfate. *Proc. Natl. Acad. Sci. USA* 105:8416–21
118. Dowd CJ, Cooney CL, Nugent MA. 1999. Heparan sulfate mediates bFGF transport through basement membrane by diffusion with rapid reversible binding. *J. Biol. Chem.* 274:5236–44
119. Geng Y, Dalhaimer P, Cai S, Tsai R, Tewari M, et al. 2007. Shape effects of filaments versus spherical particles in flow and drug delivery. *Nat. Nanotechnol.* 2:249–55
120. Ruggiero A, Villa CH, Bander E, Rey DA, Bergkvist M, et al. 2010. Paradoxical glomerular filtration of carbon nanotubes. *Proc. Natl. Acad. Sci. USA* 107:12369–74
121. Pluen A, Netti PA, Jain RK, Berk DA. 1999. Diffusion of macromolecules in agarose gels: comparison of linear and globular configurations. *Biophys. J.* 77:542–52
122. Jain RK, Forbes NS. 2001. Can engineered bacteria help control cancer? *Proc. Natl. Acad. Sci. USA* 98:14748–50

Annual Review of Chemical and Biomolecular Engineering

Volume 2, 2011

Contents